

# Magnetic Resonance Imaging and Clinical Features in Acute and Subacute Myelopathies

Stefan Weidauer<sup>1</sup> · Marlies Wagner<sup>2</sup> · Michael Nichtweiß<sup>3</sup>

Received: 6 March 2017 / Accepted: 7 June 2017 / Published online: 30 June 2017  
© Springer-Verlag GmbH Germany 2017

**Abstract** Differential diagnosis of acute and subacute transverse myelopathy includes inflammatory, infectious, vascular, metabolic and paraneoplastic etiologies. Information on the diagnostic approach to transverse myelopathy with regard to daily clinical practice is provided. The differentiation between five lesion patterns on magnetic resonance imaging (MRI) in myelitis may be helpful: (1) longitudinal extensive transverse myelitis, (2) short segment ovoid or peripherally located, (3) “polio-like”, (4) granulomatous and (5) segmental with rash. A correlation with these imaging features is supported if the clinical course and neurological symptoms are known. Although the mean interval from onset to nadir of symptoms in spinal cord infarction is 1 h, an overlap with a fulminant course of myelitis is possible, and impaired diffusion may also occur in acute inflammatory processes. As a result, laboratory testing, including aquaporin-4 antibodies and cerebrospinal fluid analysis, is crucial for the correct interpretation of imaging findings. Moreover, the discrimination of acute complete and acute partial transverse myelitis is advantageous in order to identify diverse entities, the latter often being a precursor to multiple sclerosis. Additional brain imaging is mandatory in suspected demyelinating, infectious, neoplastic and systemic autoimmune disease. A symmetrical lesion pattern restricted to individual tracts

or dorsal columns indicates subacute combined degeneration of the spinal cord and, in addition to deficiency syndromes, a paraneoplastic etiology should be considered.

**Keywords** Myelopathy · Myelitis · Magnetic resonance imaging · Spinal cord infarct · Spinal vascular disease

## Introduction

The differential diagnosis of progressive neurological syndromes due to spinal cord dysfunction encompasses a broad spectrum of different etiologies [1–3]. This review deals with morphological equivalents of clinical spinal cord syndromes as far as depictable on MRI, summarized under the umbrella term myelopathy [4], and information on the identification and analysis of MRI features with special regard to neurological symptoms will be discussed. Due to specific treatment options, correct categorizing of these lesions is crucial. The first step is to immediately exclude extradural compression in an emergency setting (see Table 1; [1, 2]). The spectrum of acute and subacute transverse myelopathy includes vascular, inflammatory, infectious, metabolic, toxic, neoplastic and paraneoplastic etiologies [1]. Although specific neuroradiological findings are well defined in several spinal cord pathologies, there is some overlap of lesion patterns [3, 5, 6]. Therefore, detailed information on onset and course of neurological symptoms is essential for the correct interpretation of imaging features [1, 7]. Additional information necessary to make the right diagnosis includes cerebrospinal fluid (CSF) analysis, serum inflammatory markers as well as microbiological serology [1, 8]. Moreover, cranial MRI is essential if systemic central nervous system (CNS) involvement is sus-

✉ Stefan Weidauer  
stefan.weidauer@sankt-katharinen-ffm.de

<sup>1</sup> Department of Neurology, Sankt Katharinen Hospital, Teaching Hospital of the Goethe University, Frankfurt, Seckbacher Landstraße 65, 60389 Frankfurt/Main, Germany

<sup>2</sup> Institute of Neuroradiology, Goethe University, Frankfurt, Germany

<sup>3</sup> Wismar, Germany

**Table 1** Differential diagnosis of acute and subacute spinal cord symptoms

1. Extradural	<i>A) Space occupying lesions</i>
	Neoplastic
	Medial disc herniation
	Spinal canal stenosis
	Spontaneous epidural hematoma (EDH)
	Spinal trauma (contusion, compression, EDH)
	<i>B) Inflammatory diseases</i>
	Epidural abscess
	Spondylodiscitis
	2. Intradural
Extra-/intramedullary tumor, meningioma, neoplasma	
<i>B) Spinal AVM</i>	
Dural fistula	
Intra-/perimedullary AVM	
Cavernoma	
<i>C) Inflammatory diseases (subdural, subarachnoid, intramedullary)</i>	
Myelitis	
Polyradiculitis (e. g. Guillain Barré syndrome)	
<i>D) Metabolic and toxic etiologies</i>	
SCDSC	
<i>E) Spinal cord infarction</i>	
<i>F) Post radiation myelopathy</i>	

pected, e. g. clinical isolated syndrome (CIS) in assumed multiple sclerosis (MS) [1, 5, 6, 9–11].

Diagnostic criteria for acute transverse myelitis (ATM) were established by the Transverse Myelitis Consortium Working Group (TMCWG) in 2002 [12]. These include appropriate neurological symptoms reaching maximum intensity within a time interval ranging from 4 h up to 21 days after onset. Inflammatory etiologies need to be demonstrated by pathological CSF findings with pleocytosis and elevated immunoglobulin and/or pathological contrast en-

hancement of the lesion on post-contrast (pc) T1-weighted images (WI). From a clinical point of view, the distinction between acute complete transverse myelitis (ACTM) and acute partial transverse myelitis (APT) is helpful, since different entities could be classified (see Table 2; [6, 10, 13]). Exclusion criteria for idiopathic as well as disease-associated ATM include: a history of radiation of the spine, perimedullary abnormal flow voids suggestive of spinal arteriovenous malformation (AVM), and abrupt onset of neurological deficits suspicious for vascular disorders, e. g. spinal cord infarction (SCI) [6, 12].

## Vascular Diseases

### Spinal Cord Vascular Anatomy

The spinal cord is supplied by radiculomedullary arteries originating from the vertebral artery (VA) and the posterior intercostal artery and may split in an anterior and a posterior radicular artery (RA) [14–17]. The thoracolumbar spinal cord including the conus medullaris is fed by a dominant anterior RA, i. e. arteria radicularis magna (syn.: arteria of Adamkiewicz), and the pelvic arteries and lateral sacral vessels arising from the internal iliac artery may potentially also contribute to cord perfusion. Whereas the anterior RA feeds the anterior spinal artery (ASA), the posterior RA supplies the pial plexus surrounding the spinal cord (vaso-corona) and the dual posterior and posterolateral spinal arteries (PSA/PLSA) [14–17]. In addition to the ASA and PSA territories, two further medullary arterial systems can be differentiated [15, 16]:

1. The intrinsic system represented by the sulcal spinal (syn.: sulcocommissural) arteries (SSA) originating alternately from the ASA to the right and left side of the cord

**Table 2** Acute transverse myelitis (ATM)

	ACTM	APT/short segmented
Clinical findings	Bilateral prominent paresis Symmetrical sensation deficits Definable sensory level Autonomic disturbances, e. g. bladder/bowel dysfunction	Possible mild motor symptoms Mild unilateral/asymmetrical sensation deficits Facultative autonomic disturbance, e. g. bladder dysfunction
MRI	Often LETM (extension $\geq 3$ vertebral segments)	Extension $\leq 2$ vertebral segments
CSF	Pleocytosis OCB often negative	Pleocytosis, often $< 50$ cells OCB often positive
Clinical course over 5 years	Relapse: 2% More incomplete remission	Definite MS: ca. 30%

Exclusion criteria for ATM: perimedullary flow voids, history of spine radiation, abrupt onset suspicious for ischemia

Inclusion criteria for ATM: progression from onset to nadir of symptoms within 4 h to 21 days; exclusion of space occupying lesion, extra-/subdural inflammatory or infectious process

ACTM Acute complete transverse myelitis, APTM acute partial transverse myelitis, CSF cerebrospinal fluid, LETM longitudinal extensive transverse myelitis, OCB oligoclonal bands

2. An extrinsic system represented by numerous small perforating arteries originating from the vasocorona and the PSA and PLSA

### Spinal Cord Infarction

In contrast to cerebral stroke, spinal cord ischemia is rare and accounts for less than 1% of all infarcts [18–21]. Unlike the sudden onset of symptoms in cerebral stroke, neurological deficits due to SCI typically manifest over a time period of 30–45 min with radicular, e. g. belt-like acute pain representing the precursor [19, 22]. Although the median time interval from onset to nadir of symptoms was 1 h, it is worth mentioning, that the mean of 7.8 h reported by Nedeltchev et al. [22] exhibits large variance, resulting in an overlap with a fulminant course of ATM [12]. Therefore, the lower time limit of 4 h for the development of maximum deficits after symptom onset in ATM does not exclude SCI. The overlapping time courses of maximum deficits underline the importance of considering additional clinical data and CSF analysis. Moreover, while the absence of contrast enhancement and restricted diffusion on diffusion weighted imaging (DWI) are indeed typical for SCI [19, 23–25], these imaging features may also be present in a fulminant course of ATM [6, 23, 26].

The etiology of SCI is heterogeneous and despite an extensive diagnostic work-up in 24% of infarcts, the etiology remains unclear [18–20]. While in younger patients VA dissection [27–32], vasculitis, antiphospholipid antibody syndrome and several rare etiologies such as fibro cartilaginous embolism [33, 34], surfers myelopathy [35, 36], drugs, e. g. cocaine, and sickle cell disease may cause SCI, in the elderly aortic diseases like arteriosclerosis, dissection and aneurysm repair are considerable risks for medullar ischemia [19, 20, 37]. Further etiologies include systemic hypotension, cardiac failure, spinal scoliosis surgery and infiltrative periradicular procedures [38]. Due to spinal cord vascularization and infarct topography, different transverse spinal cord syndromes with specific imaging pattern may occur (see Table 3; [3, 18–20, 39]).

The most common clinical feature in SCI is ASA syndrome with bilateral extensive transverse spinal cord lesions sparing PSA territories (see Fig. 1; Table 3; [18–20]). If segmental duplication of the ASA is present, SSA syndrome may occur [15, 40]. MRI exhibits a unilateral cord lesion and, in contrast to the Brown-Séquard syndrome [39, 41–43] representing a hemispinal cord lesion, the posterior columns are spared (see Table 3; [27]). Possibly due to sufficient collateralization, circumscribed infarcts in the PSA territory are rare [29, 44, 45]. Although imaging features may be similar to subacute combined degeneration of the spinal cord (SCDSC), e. g. caused by vitamin B12 defi-

ciency [46–49], the clinical course of SCI with abrupt onset of ataxic gait and impaired proprioception helps to distinguish SCI from SCDSC (see Table 3). Entire cross-sectional damage of the spinal cord often occurs in the lower thoracic and thoracolumbar spinal cord caused by aortic pathologies with consecutive flow impairment or occlusion of the artery of Adamkiewicz [17–20, 37].

Due to the higher vulnerability of the motoneurons in anoxia, hemodynamic infarcts at the watershed between the intrinsic and extrinsic system most often manifest in the anterior horns [50]. Characteristic lesion patterns on T2 WI depict the “snake eye” or “owl’s eye” configuration [30, 31]. If the cervical spinal cord is affected, neurological examination shows flaccid, often symmetrical palsies of the proximal muscles of the upper extremities, so-called man-in-the-barrel syndrome [51, 52]. However, a “snake eye” or “owl’s eye” lesion pattern is not specific for a vascular origin. Other diseases affecting the motoneurons in the anterior horns such as lower motoneuron diseases [53], e. g. spinal muscle atrophy (SMA) [53], Hirayama disease [54, 55], Hopkins disease [56] and infectious etiologies, e. g. poliomyelitis or tick-borne encephalomyelitis (see below), may also induce this type of lesion pattern [3, 57–60].

As in acute cerebral ischemia, DWI is the imaging method with the highest sensitivity for depicting SCI [19, 24, 25]. However, one should bear in mind that ATM may also show restricted diffusion [23, 26]. Conversely, T2 WI may be negative in SCI, especially within the first 15 h after symptom onset [61, 62]. However, in the further course of SCI, up to 98% of patients will show hyperintense signal changes on T2 WI, and typically in the second week after SCI additional vertebral body infarcts may be visible [19, 20].

### Vascular Malformation

Neurological manifestations of spinal vascular malformations are variable, including acute complete transverse spinal cord syndrome due to hematomyelia [21]. Spinal dural AV fistula fed by radiculomeningeal branches should be regarded as a separate type of shunting lesion and not be included in the (true) AV malformations. AVM supplied by radiculomedullary or radiculopial arteries result in pial cord AVM with two subtypes, i. e. (1) glomerular (plexiform or nidus type) and (2) fistulous pial AVM, which may show high shunting (macrofistula) or low shunting (microfistula) volume [63]. Spinal cord cavernoma represents a non-shunting spinal vascular malformation. However, a detailed description of spinal AVM goes beyond the scope of this review and is published elsewhere [63]. Due to venous overloading in dual AV fistula, the spinal cord drainage is compromised resulting in venous congestion [63, 64]. MRI exhibits cord swelling with partially homogeneous

**Table 3** Neurological syndromes, clinical findings and lesion patterns

Neurological syndrome	Clinical findings	Lesion pattern
Spinal sulcal artery (syn.: sulcocommissural)	Ipsilateral spastic (hemi-)paresis, contralateral dissociated sensation deficits (loss of pain and temperature sense)	
Centromedullary (syn.: ASA syndrome)	Flaccid paresis at the lesion level and (spastic) para- or tetraparesis below, bilateral sensation deficits (loss of pain and temperature sense), bladder and bowel dysfunction, facultative vegetative dysfunctions and Horner's syndrome	
Complete transverse spinal cord syndrome of the artery of Adamkiewicz	Flaccid paresis at the lesion level and (spastic) para- or tetraparesis below, (in-) complete loss of sensation below, bladder and bowel dysfunction (see also Table 4)	
"Man-in-the-barrel"	Bilateral flaccid proximal paresis of the upper limbs, no sensation deficits (see also Table 4)	

**Table 3** Neurological syndromes, clinical findings and lesion patterns (Continued)

Neurological syndrome	Clinical findings	Lesion pattern
Posterior spinal artery	Disturbance of proprioception (light touch and vibration sense), ataxic gait disturbance	
Brown-Séquard (hemispinal cord)	Ipsilateral spastic paresis, dissociated sensation deficits (ipsilat.: disturbance of proprioception; contralat.: loss of pain and temperature sense)	
SCDSC	Bilateral disturbance of proprioception, ataxic gait disturbance, facultative spastic paraparesis	

ASA Anterior spinal artery, SCDSC subacute combined degeneration of the spinal cord, 1 radiculomedullary artery, 2 anterior radicular artery, 3 posterior radicular artery, 4 anterior spinal artery, 5 sulcal spinal (syn.: sulcocommissural) artery, 6 posterolateral spinal artery, 7 posterior spinal artery, 8 vasocorona, 9 dorsal root ganglion

hyperintense signal changes on T2 WI and characteristic perimedullary flow voids due to vein enlargement (see Fig. 2; [65]). If shunt volume is small, only pc T1 WI may be able to depict pathological perimedullary vascular structures beside inhomogeneous intramedullary contrast enhancement due to venous congestion. While clinical symptoms are often slowly progressive over years, acute deterioration due to additional ischemic complications within the congestive myelopathy may occur [64, 66].

Neurological findings caused by spinal cord cavernoma range from slight radicular sensation deficits to acute, progressive or recurrent myelopathies with transverse spinal cord syndromes due to intralesional bleeding with different grades of perifocal reaction (see Fig. 3; [63]). Be-

side space occupying effects, toxic hemorrhagic products as well as perifocal capillary proliferation and vessel dilation may be responsible for progressive symptoms [63]. In line with imaging features of cerebral cavernoma, spinal MRI shows circumscribed, often clearly defined lesions with a hypointense rim caused by hemosiderin deposits and inhomogeneous hyperintense intralesional signal on T2 WI depending on different stages of hemorrhages, the so-called mulberry appearance [6, 63].





**Fig. 1** Anterior spinal artery syndrome. Sagittal T2 WI (a) showing a pencil-like longitudinal extensive hyperintense lesion ventrally accentuated in the cervical spinal cord (arrows). Axial T2 WI (b–d) exhibit bilateral partially symmetrical hyperintense signal conversion beginning in the anterior horns (b–d; arrow) and sparing of the posterior spinal artery territory (d; arrowhead)

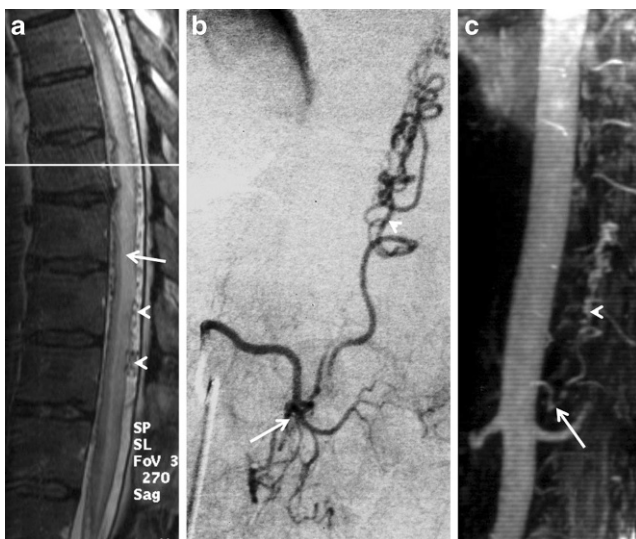


**Fig. 2** Sagittal T2 WI (a) demonstrating venous congestion of the spinal cord with swelling (arrow) and perimedullary flow voids (arrowhead) due to varicose enlargement of overloaded vein (b: selective DSA; c: contrast enhanced MRA; arrowhead) caused by dural arteriovenous fistula (b, c: arrow)

## Inflammatory Lesions

The underlying etiologies of ATM cover a broad spectrum. Therefore, differentiation between ACTM and APTM is a helpful concept, since different disease entities could be distinguished, the latter often being the initial manifestation of MS (see Table 2; [1, 2, 6, 10]). Knowledge of clinical course and neurological symptoms facilitates the correlation of imaging features to certain etiologies [1, 3, 59]. In children, however, the differentiation between ACTM and APTM is less helpful compared to adult patients regarding the course of the disease and final diagnosis [13, 67].

APTMs often show mild neurological deficits and 5-year follow-up will exhibit progression to definite MS in up to 30% of patients [6, 10, 68]. MRI typically shows peripherally located ovoid lesions with hyperintense signal changes on T2 WI and the longitudinal extension is shorter than two vertebral segments [5, 6, 69–71]. In contrast, longitudinal extensive transverse myelitis (LETM) extends over at least three vertebral segments, involves complete or most of the cross section of the spinal cord and is associated with distinct neurological deficits ranging up to para- or tetraplegia (see Table 2; [72, 73]). Laboratory analysis should include specific autoimmune antibodies [74–76]. The diagnosis of idiopathic ATM requires exclusion of systemic autoimmune disease (SAD) [12] such as systemic lupus erythematosus (SLE) [77], Sjögren's syndrome (SS) [78], Behçet's disease [79, 80], as well as known agents associated with infectious etiology [74, 81]. Additional cerebral imaging is required to depict possible cerebral lesions in suspected SAD [1–3, 5, 6, 12, 69]. The distinction of five different lesion patterns on MRI might be helpful in daily clinical practice:

1. LETM
2. Short segment ovoid or peripherally located
3. “Polio-like”
4. Granulomatous, nodular
5. Segmental with rash [3, 59].

## Longitudinal Extensive Transverse Myelitis (LETM)

The definition of LETM was established by Wingerchuk et al. [72] in 2007 to differentiate spinal cord involvement in neuromyelitis optica (NMO) from MS. Conversely, etiologies of LETM show a wide range, including inflammatory diseases such as SLE, SS, Behçet's disease, sarcoidosis and acute disseminated encephalomyelitis (ADEM), as well as infectious and parainfectious disorders (see Table 4) and the differential diagnosis includes vascular, neoplastic and nutritional causes (see Table 1; [5, 6, 11, 73, 74, 82–85]). Aquaporin-4 antibodies (AQP4-ab) discovered in 2004 are highly specific for NMO [72]. Besides clinical syndromes or MRI lesions related to the optic nerves and the spinal

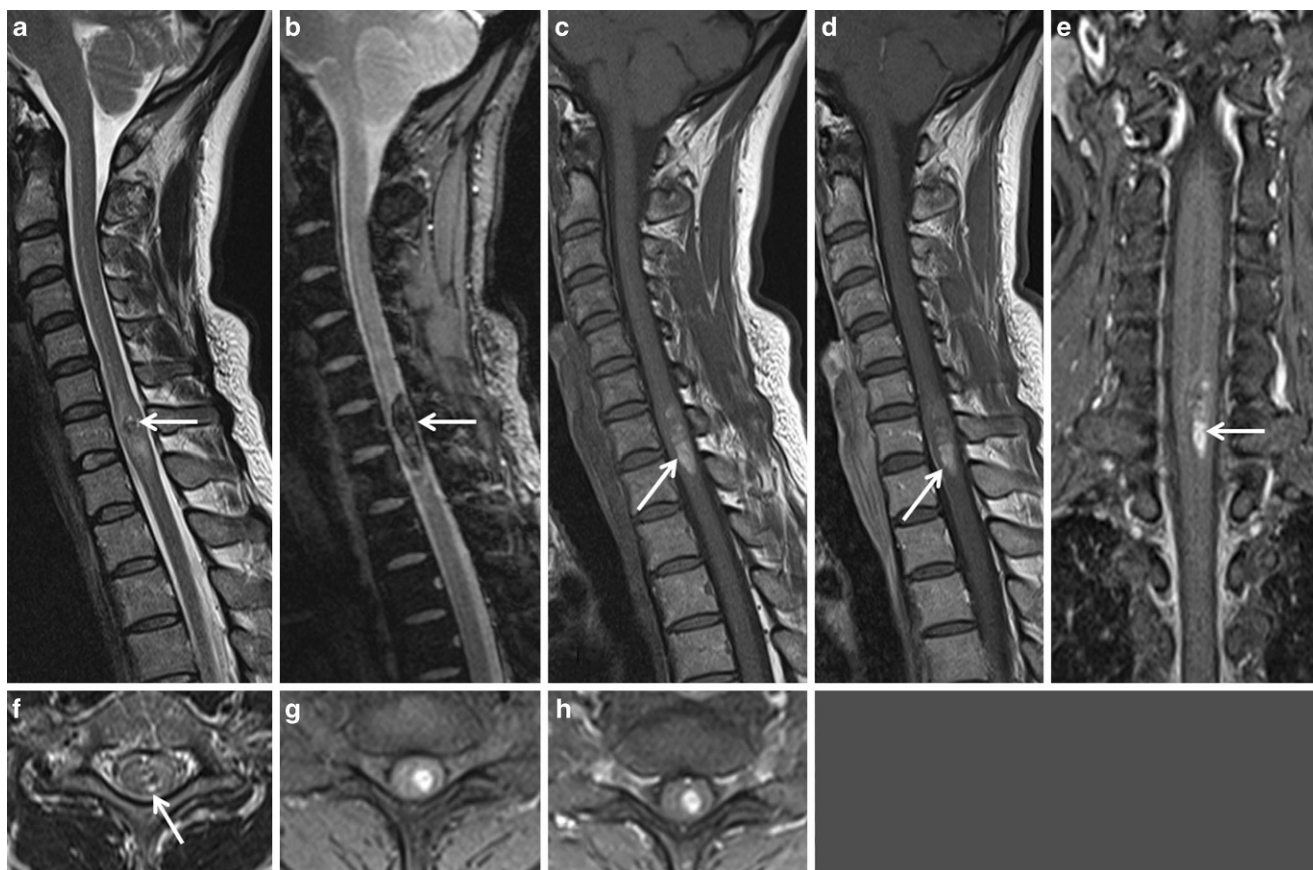


**Fig. 3** Spinal cavernoma in a 45-year-old woman suffering from hypoesthesia in the left C7 and C8 dermatome. T2 WI (a: sagittal; f: axial) showing an intramedullary space occupying lesion at the level C7 paramedian left-sided with inhomogeneous signal abnormalities (mulberry appearance; *arrow*) and hypointense signal changes on sagittal T2\* WI (b; *arrow*). T1 WI (c: sagittal; g: axial) exhibit subacute bleeding with hyperintense signal changes (*arrows*) without enhancement on pc T1 WI (d: sagittal; e: coronal (*arrow*); h: axial).

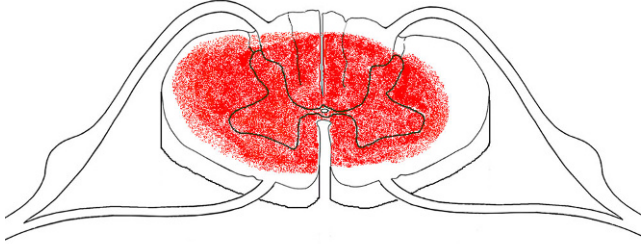
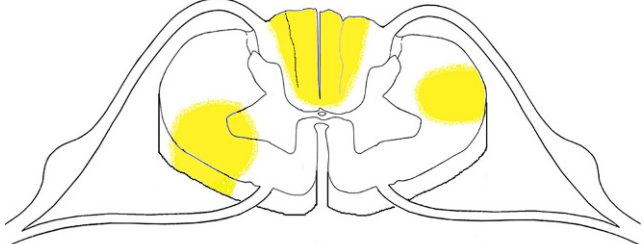
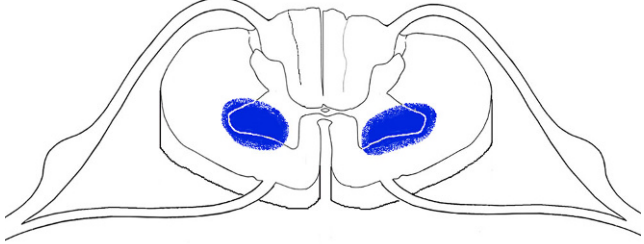
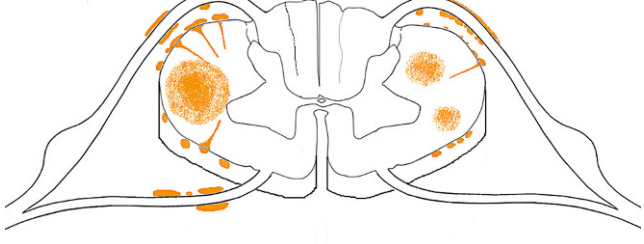
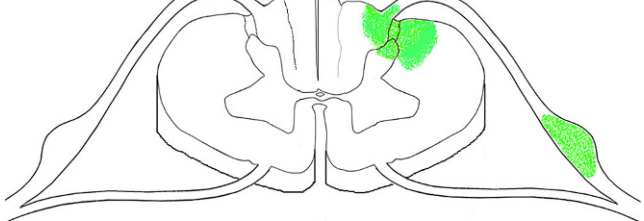
cord, additional lesions in the brainstem, the diencephalon and other specified cerebral regions may occur [86, 87], and new diagnostic criteria were defined by Wingerchuk et al. in 2015 resulting in the unifying term NMOSD spectrum disorders (NMOSD) [88]. There seems to be a relationship between cerebral involvement and lesion pattern and the distribution of AQP4 [89].

Whereas evidence of AQP4-ab in LETM proves the diagnosis of NMOSD and excludes MS, the absence of AQP4-ab or NMOSD with unknown AQP4-ab status require specific MRI features as well as core clinical symptoms [88]. Imaging criteria include the predominance of grey matter involvement in at least 70% of the centrally located lesions and contrast enhancement without a specific pattern should be present [86–88]. Rostral extension into the brainstem with special regard to the area postrema, cord swelling and T1 hypointensity [88] of regions with hyperintense signal changes on T2 WI, bright spotty lesions [90] and linear lesions with extension to the area postrema are additional imaging features (see Fig. 4; [91]). However, Flanagan et al. [92] reported on 25 (14%) of 176 patients suffering from short transverse myelitis (STM) with extension below three

vertebral segments positive for AQP4-ab. Follow-up over a 5.4-year period revealed relapse in 92% [92, 93]. In contrast to STM negative for AQP4-ab, a central lesion pattern, T1 hypointensity and negative OCB are typical in NMOSD related STM [92, 93]. Knowledge of this imaging precursor in NMOSD is important, since the therapeutic strategies in MS and NMOSD differ [93]. Whereas immune-modulating substances are recommended promptly in CIS or MS, such therapies are potentially harmful in NMOSD [92, 93].

T1 hypointensity, which is never seen in MS lesions, may reflect the more complicated clinical course in NMOSD with incomplete remission and persistent neurological symptoms (see Fig. 4; [89, 90]). One reason for this is the different target of autoimmune-related inflammatory processes in MS and NMOSD. Histological examination in NMOSD revealed the destructive nature of lesions with necrotizing demyelination and cavitation and thickened vessel walls, strongly suggesting autoimmune astrocytopathy [89]. AQP4 is concentrated on perivascular astrocytic foot processes at the blood–brain barrier, subpial and subependymal regions and a vasocentric pattern of im-

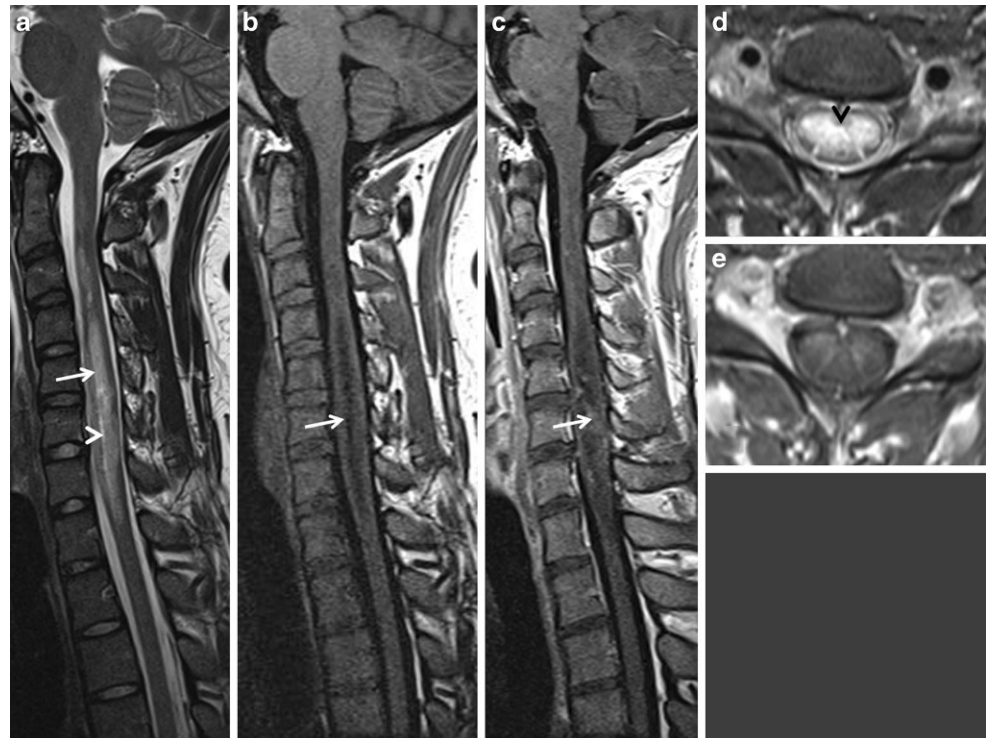
**Table 4** Acute transverse myelitis: lesion type on MRI, etiology and lesion pattern

Lesion type	MRI findings	Etiology	Lesion pattern
1. Longitudinal extensive transverse myelitis (LETM)	<ul style="list-style-type: none"> <li>≥3 Vertebral segments</li> <li>Predominately grey matter</li> <li>Facultative T1 hypointensity</li> <li>Often swelling</li> <li>Enhancement when present: patchy, extensive</li> </ul>	<ul style="list-style-type: none"> <li>NMOSD (AQP4-ab?)</li> <li>SAD</li> <li>ADEM</li> <li>Viral, bacterial, parasitic</li> <li>Idiopathic (see also Table 3)</li> </ul>	
2. Short segment ovoid or peripherally located	<ul style="list-style-type: none"> <li>&lt;2 Vertebral segments</li> <li>Predominately white matter</li> <li>Possible slight swelling</li> <li>Enhancement when present: homogeneous, eccentrically</li> </ul>	<ul style="list-style-type: none"> <li>CIS (MS)</li> <li>Other (e. g. NMOSD, Behçet's disease; the exact localisation could differ)</li> </ul>	
3. "Polio-like"	<ul style="list-style-type: none"> <li>Anterior horns grey matter</li> <li>Often symmetrical T2 hyperintensities</li> <li>"Snake/owl's eyes"</li> </ul>	<ul style="list-style-type: none"> <li>Viral: poliomyelitis, tick-borne, EV D68, picorna- and flaviviridae;</li> <li>Atopic (see also Table 3)</li> </ul>	
4. Granulomatous nodular	<ul style="list-style-type: none"> <li>Variable longitudinal extension</li> <li>Swelling</li> <li>Enhancement: nodular eccentric or diffuse nodular, facultative pial and radicular</li> </ul>	<ul style="list-style-type: none"> <li>Parasitic</li> <li>Sarcoidosis</li> <li>Bacterial (e. g. tuberculosis, lues, other)</li> <li>DD: meningeosis neoplastica</li> </ul>	
5. Segmental with rash	<ul style="list-style-type: none"> <li>White (and grey) matter entry zone of dorsal root</li> <li>Uncommonly hemispinal cord lesion</li> </ul>	VZV	

*ADEM* Acute disseminated encephalomyelitis, *AQP4-ab* aquaporin 4 antibody, *CIS* clinically isolated syndrome, *EV* enterovirus, *LETM* longitudinal extensive transverse myelitis, *MS* multiple sclerosis, *NMOSD* neuromyelitis optica spectrum disorders, *SAD* systemic autoimmune disease, *VZV* varicella zoster virus



**Fig. 4** Neuromyelitis optica spectrum disorders (NMOSD). T2 WI (a: sagittal; d: axial) showing longitudinal extensive transverse myelitis (a; arrow) with bright spotty lesions (a, d: arrowhead) and cord swelling; hypointense signal changes on T1 WI (b; arrow) and patchy inhomogeneous enhancement on pc T1 WI (c: sagittal; e: axial) in a young woman suffering from fulminant progressive tetraparesis



munoglobulin G (IgG) deposition in NMO lesions was demonstrated [89].

LETM may be the initial manifestation of SAD in 16.5% of cases [6, 77]. On the other hand, LETM in SAD may also be part of NMOSD, underlining the necessity for AQP4-ab testing as an essential step in the diagnostic work-up of LETM [88, 94]. Kitley et al. [75] reported on 76 patients suffering from LETM with 44 patients (58%) testing positive for AQP4-ab, clearly reflecting the majority of NMOSD in LETM. Moreover, an additional five patients negative for AQP4-ab fulfilled the criteria for NMOSD.

SLE associated myelitis could be divided in two subtypes preferentially affecting grey or white matter [77]. Patients with grey matter lesions often show rapid clinical progression to nadir <6 h with pronounced irreversible para- or tetraparesis and bladder dysfunction [77]. An additional ischemic component is thought to be part of the pathogenesis with perivascular inflammation, and DWI may show restricted diffusion in correlation to ischemic necrosis and infarction seen on histological studies [6, 77, 89]. Fever, headache, malaise and urinary retention have been identified as short clinical prodromes prior to irreversible motoric deficits [77]. The second subtype preferentially affecting white matter of the spinal cord typically shows a more subacute onset with mild para- or tetraparesis, spasticity, hyperreflexia and bladder dysfunction. Altogether, 55% of patients had a history of optic neuritis, 57% were positive for NMO-IgG and DWI was negative (see Fig. 5; [77]).

In the NMOSD subgroup negative for AQP4-ab, additional testing for antibodies directed to myelin oligodendrocyte-glycoprotein (MOG-IgG) is required [95–98]. Patients negative for AQP4-ab and positive for MOG-ab generally showed a favorable monophasic disease course and additional cerebral NMOSD lesions were absent [10]. These patients showed a trend towards younger age, and more often presented with coincident optic neuritis and positive OCBs on CSF analysis. During the course of the disease, a more MS-like lesion pattern on cerebral MRI may be seen [95, 96, 98]. However, the differential diagnosis should include a site restricted spinal form of ADEM [3, 11].

In a pediatric population, up to 40% of patients suffering from LETM showed clinical signs and serological evidence of previous and frequently viral infection, while the rate of parainfectious etiology varies between 6% and 45% in adults [5, 6]. Differentiation between infectious and parainfectious ATM is difficult and viral agents are more common than fungal or bacterial causes (see Fig. 6; [3, 59]). A fulminant clinical course of spinal involvement within some hours may occur. This is probably not due to an extraordinary virulence of certain agents, but to an abnormal immunological response in microbial superantigen-mediated infection [81]. However, most commonly, neuronal damage is a consequence of molecular mimicry between microbial antigens and most likely neuronal cell wall components [81]. Rapid progressive LETM in bacterial meningitis is a rare complication due to bacterial cord invasion via ve-

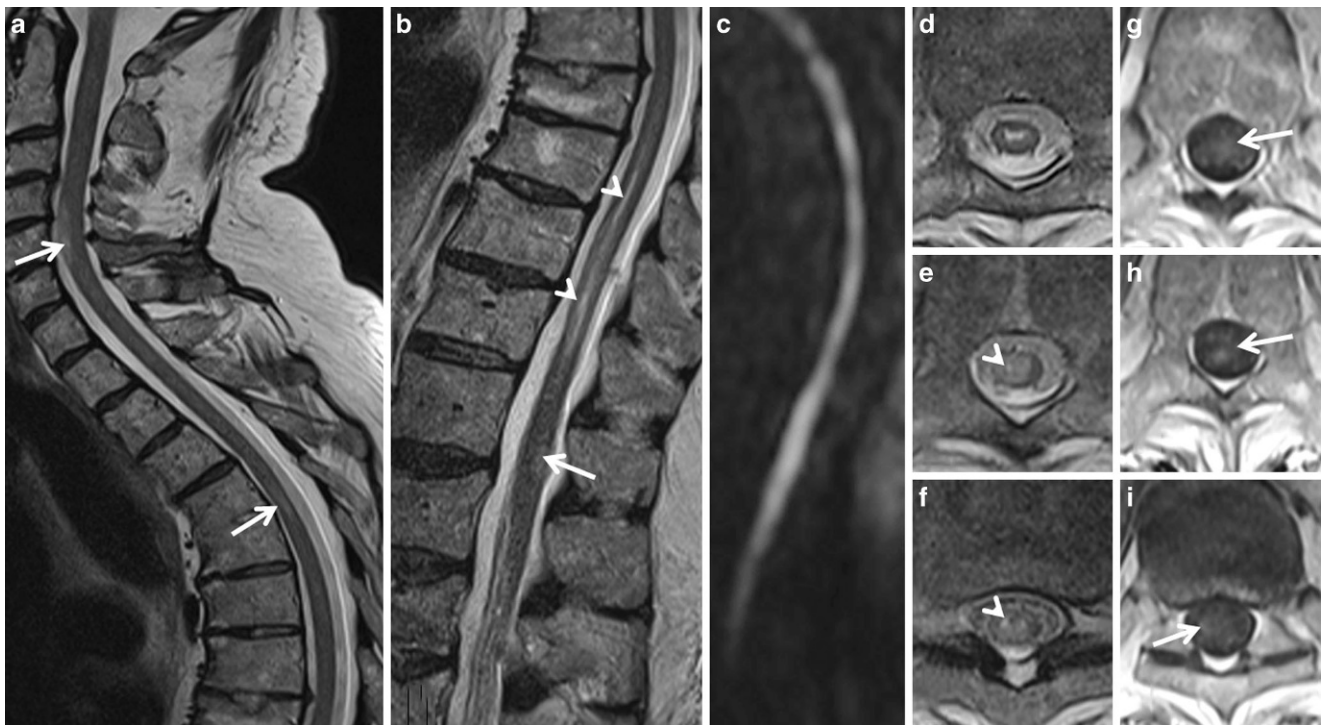
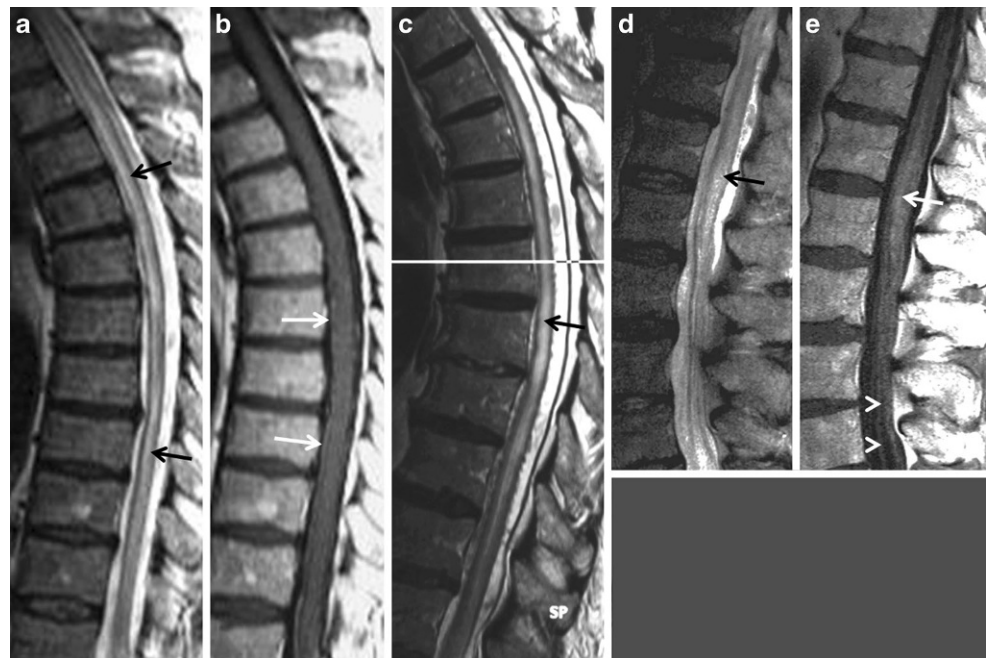


**Fig. 5** Longitudinal extensive transverse myelitis (LETM) in a 73-year-old man with progressive paraparesis within 10 days and a history of recurrent optic neuritis in systemic lupus erythematosus (SLE) and NMOSD. T2 WI (a, b: sagittal; d–f: axial) demonstrating several focal hyperintense lesions (a, b: arrow) and additional LETM with bright spotty lesions (b, d–f: arrowhead), especially in the grey matter of the spinal cord. T1 WI pc (g–i, axial) exhibiting inhomogeneous stained intramedullary enhancement (arrow).

**Fig. 6** Sagittal T2 WI (a) showing parainfectious LETM due to septicemia after urogenital infection with inhomogeneous intramedullary hyperintense signal changes (arrow) in the entire thoracic cord in a 75-year-old man suffering from rapid progressive paraparesis within 24 h. T1 WI pc (b) revealing slight leptomeningeal enhancement (arrow). c–e: LETM in bacterial meningomyelodiscitis (pneumococcus infection) causing paraplegia within 3 days. T2 WI (c, d: sagittal) demonstrating distinct hyperintense spinal cord (arrow) and T1 WI pc (e) exhibiting confluent intramedullary (arrow), leptomeningeal and radicular (arrowhead) enhancement



nous pathways, and additional infarcts, hematomyelia and abscess are further dramatic consequences (see Fig. 6; [99]).

Interestingly, venous hypertensive myelopathy subsequent to cervical spondylosis may mimic imaging features of LETM [100]. Flanagan et al. [101] emphasized trans-

verse pancake-like gadolinium enhancement of the spinal cord caudally to the site of maximal spinal stenosis as a diagnostic clue that spondylosis is the cause of myelopathy.



**Fig. 7** Multiple sclerosis (MS). T2 WI (a: sagittal; c: axial) showing a hyperintense ovoid lesion in the lateral circumference of the cervical cord (c, *arrow*) with partially homogeneous enhancement on pc T1 WI (b: sagittal; d: axial; *arrow*) in a young man suffering from incomplete right-sided Brown–Séquard syndrome

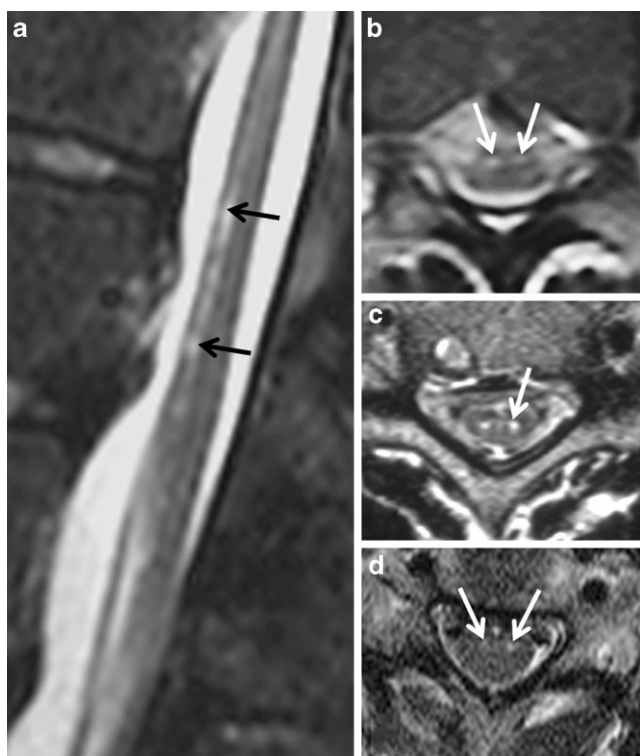


**Fig. 8** “Polio-like” lesion pattern: 28 year-old-woman with flaccid paraparesis due to tick-borne myelitis. T2 WI (a: sagittal; b: axial) demonstrating hyperintense lesions in the projection of the anterior horns of the spinal cord (*arrows*). c and d: Similar imaging features (“snake eyes” or “owl’s eyes”) also visible on axial T2 WI in a patient suffering from spinal cord infarction with man-in-the-barrel syndrome (c; *arrow*) and in a 72-year-old woman with spinal muscle atrophy (SMA; d, *arrows*)

### Short Segment Ovoid or Peripherally Located

These lesions are predominately located in the white matter, exhibiting broad contact to the cord surface with possible swelling in the acute phase (see Fig. 7; [1, 3, 6, 69–71]). The longitudinal extension is typically shorter than two vertebral segments and T1 hypointensity is very uncommon. The prototype of neurological manifestation is APTM, [10, 13] suspicious for CIS as the spinal precursor of MS [13, 68, 69, 102]. In the acute stage, these lesions often show homogeneous or eccentric enhancement on pc T1 WI, and focal atrophy may be present in the chronic stage [69, 71, 103, 104]. Early in the course of MS, the cervical spinal cord is preferentially affected and biomechanical stress with special regard to lateral cord circumference via anchorage of the ligamenta denticulata and extensive mobility of the cervical spine might be a promoting process [105]. In contrast to MS, STM in the beginning of NMOSD mentioned above discloses a more often central location with prominent involvement of the grey matter, relationship to the central canal and possible T1 hypointensity. The identification of this differential diagnosis is important due to the disparity of treatments [3, 92, 93].

### “Polio-like”

Besides prototypical poliovirus, other picorna- and flaviviridae affecting in particular motoneurons in the anterior horns may also show this lesion pattern, often exhibiting symmetrical hyperintense signal changes on T2 WI (see Fig. 8; [3, 57]). During the enterovirus D68 outbreak of 2014, Maloney et al. [57] performed an MRI study on affected chil-



**Fig. 9** Granulomatous lesion pattern: T2 WI (**a, b**: sagittal; **e**: axial) disclosing extended, centrally accentuated hyperintense lesion (*arrow*: **a, b**) of the cervical and thoracic cord and diffuse leptomeningeal (*arrow*: **c, d, g**) and partially nodular intramedullary (*arrowhead*: **c, f**) enhancement on pc T1 WI (**c, d**: sagittal; **f, g**: axial) in eosinophil (**h**: cerebrospinal fluid) meningomyeloradiculitis caused by neurotoxocarisis resulting in progressive paraparesis within 3 days

dren suffering from acute flaccid paralysis. MRI disclosed longitudinal extensive lesions of the entire grey matter of the spinal cord and, in the subacute stage, lesions restricted to the anterior horn cells with enhancement of the ventral nerve roots, similar to the positive anterior cauda sign in ischemic spinal cord damage [15]. Although this lesion pattern reduces the differential diagnosis of infectious agents, it is not specific and may also occur in hemodynamic diseases caused by elective parenchyma necrosis [26, 27, 50–52], in neurodegenerative diseases affecting the lower motoneurons, e. g. SMA ([53–55] and see Fig. 8), and in Hopkin’s syndrome with focal amyotrophy after atopic myelitis [56]. Moreover, hyperintense signals on T2 WI in the anterior horns were reported at the start of NMOSD relapse [58].

### Granulomatous, Nodular

Imaging shows enhancing nodular lesions located in the leptomeninx around the spinal cord and the nerve roots, as well as intramedullary nodules, both potentially accompanied by focal edema with cord swelling [59, 73, 74]. The differen-

tial diagnosis includes bacterial agents, i. e. tuberculosis and lues, as well as parasitic infections (see Fig. 9). In addition, meningeal carcinomatosis and sarcoidosis should be considered, whereas the latter with true granuloma may exhibit hypointense signal on T2 WI with surrounding edema and homogeneous contrast enhancement (see Fig. 10; [106]). However, the discrimination between LETM in NMOSD and sarcoidosis may be challenging [84]. In a recent paper, Flanagan et al. [84] pointed out that subpial enhancement spanning at least two vertebral segments and persisting over 2 months despite high-dose corticoid treatment was suggestive of sarcoidosis, whereas ring-like or patchy enhancement was more common in NMOSD. In neurotoxocarisis as a typical parasitic infection of the CNS, the prevalently neurological manifestation is myelitis in 60% [107], underlining the advantage of additional cytological CSF analysis, which often exhibits significant eosinophilia (see Fig. 9; [108]). However, the diagnosis rests on antibody testing.



**Fig. 10** Sarcoidosis in a 25-year-old man suffering from sciatic pain of several months' standing without neurological deficits. T2 WI (a: axial) showing a hyperintense inhomogeneous lesion in the thoracolumbar region (arrow) with cord swelling and diffuse nodular (arrows: b, c), inhomogeneous leptomeningeal (b, d: arrowheads) and radicular (b, d: open arrow) enhancement on pc T1 WI



### Segmental with Rash

The characteristic infectious agent in this type of myelitis is varicella zoster virus (VZV). Since viruses persist in the dorsal root ganglia and the trigeminal and geniculate ganglia, the spinal cord lesions are located around the entry zone of the dorsal nerve roots [3, 59, 109]. Comparable to ovoid lesions mentioned above broad, contact to the cord surface is visible and Brown-Séquard syndrome represents a rare complication (see Table 3; [110]). In contrast to ischemic SSA syndrome, posterior columns are also involved, representing hemispinal cord syndrome with dissociated sensation deficits and ipsilateral spastic paresis below the affected level.

### Subacute Combined Degeneration of the Spinal Cord

In subacute combined degeneration of the spinal cord (SCDSC), the generally symmetrical lesions are confined to individual columns and certain tracts, and histology reveals primary involvement of myelin sheets in vitamin B12 and copper deficiency syndromes (see Fig. 11; [47, 48]). In addition, N<sub>2</sub>O inducing methionine synthase inactivity may also cause SCDSC [46]. Especially the centers of the dorsal and lateral columns are involved and additional brain imaging may exhibit leukoencephalopathy with confluent hyperintense signal changes on T2 WI in the centrum semiovale and neuropathy of the optic nerves with patchy enhancement on pc T1 WI [47, 48].

Vitamin E deficiency is depicted exceedingly rarely, showing similar imaging features. However, histological examination discloses axonal degeneration due to axonal neuropathy of the sensory neurons located in the spinal ganglia, comparable to axonal degeneration in Friedreich's ataxia [48]. Differential diagnosis should include paraneoplastic tractopathy exhibiting a similar lesion pattern on MRI and sometimes involvement is restricted to the corticospinal tract [6, 111, 112]. Another SCDSC mimic is vacuolar myelopathy, best known from HIV infection, where dorsal and lateral columns are preferentially affected. Enhancement on pc T1 WI may be a clue for opportunistic infection or lymphoma, whereas HIV myelitis is a more problematic radiological diagnosis and in particular neuropathological evidence is lacking [48, 113, 114]. Early deficiency treatment in SCDSC may result in complete remission of neurological symptoms and pathological imaging findings (see Fig. 11; [47, 48]). Spinal cord atrophy may be visible in the chronic stage of the disease [47, 48, 104]. A detailed description of other chronic metabolic and hereditary diseases affecting the spinal cord, e. g. adult polyglycosan body disease (PGBD) or leukoencephalopathy with brainstem and spinal cord involvement and high lactate (LBSL) is beyond the scope of this review [48, 115].

In conclusion, the differential diagnosis of acute and subacute myelopathy includes vascular, inflammatory, (para-) infectious, metabolic, toxic and paraneoplastic etiologies. The first step in the diagnostic approach to myelopathy is to exclude cord compression in an emergency setting. Due to spinal cord vascularization, different lesion types may

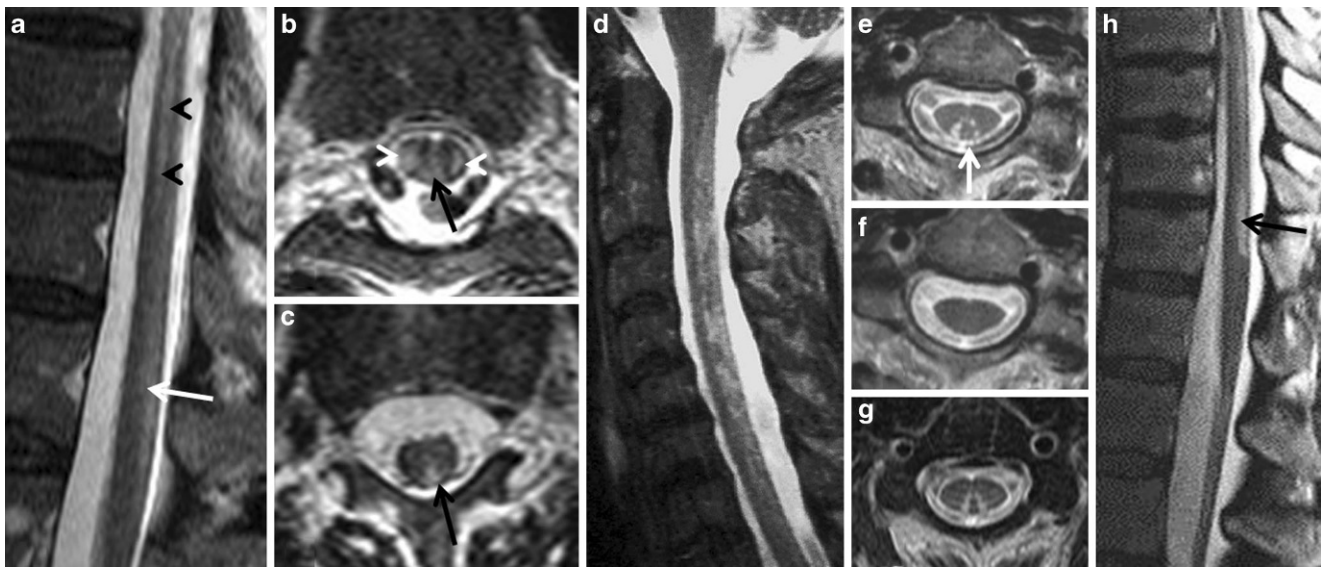


**Fig. 11** Subacute combined degeneration of the spinal cord (SCDSC). T2 WI (a: sagittal; b, c: axial) demonstrating homogeneous hyperintense signal changes of the dorsal columns (*arrow*) and the corticospinal tract (*arrowhead*) due to vitamin B12 deficiency with progressive gait disturbance. T2 WI (d: sagittal; e: axial) exhibiting patchy hyperintense signal conversion, especially in the lateral borders of the dorsal columns (e: *arrow*) in the early phase of funicular myelopathy and complete restitution after 9 months due to sufficient vitamin B12 substitution (f). g Similar imaging features in copper deficiency; h (T2 WI sagittal): SCDSC due to N<sub>2</sub>O exposure

occur in SCI. Although the mean time interval from onset to nadir of symptoms in SCI is 1 h, an overlap with a fulminant course of ATM is possible. Moreover, restricted diffusion on DWI characteristic for SCI may also be visible in acute inflammatory processes. The etiology of ATM covers a broad spectrum and, therefore, differentiation between ACTM and APTM is advantageous, since some disease entities could be distinguished, the latter often being the initial presentation of MS. A differentiation of five lesion patterns on MRI in ATM may be helpful:

1. LETM
2. Short segment ovoid or peripherally located
3. “Polio-like”
4. Granulomatous nodular
5. Segmental with rash

Correlation with these imaging features is facilitated if the clinical course and neurological symptoms are known. However, additional brain imaging is mandatory especially in suspected CIS, SAD and NMOSD. Although LETM is the typical spinal manifestation of NMOSD, STM may be the precursor of this disease underlining the necessity of AQP4-ab testing in ATM. Knowledge of these divergent imaging features in NMOSD is important due to the different therapeutic strategies in MS and NMOSD.

MRI may also provide clues suggesting myelopathies other than ATM or SCI. A symmetrical lesion pattern restricted to individual tracts or especially the dorsal columns facilitates the diagnosis of SCDSC in metabolic disorders such as vitamin B12 or copper deficiency syndromes; a

paraneoplastic etiology may also come into consideration. In addition, beside neurological features and laboratory testing, CSF analysis is crucial for the correct interpretation of spinal imaging findings. The presence of perimedullary flow voids is highly suspicious for spinal AVM with special regard to dural AV fistula, and additional venous congestion may occur.

**Conflict of interest** S. Weidauer, M. Wagner and M. Nichtweiß declare that they have no competing interests.

## References

1. Schmalstieg W, Weinschenker BG. Approach to acute or subacute myelopathy. *Neurology*. 2010;75:S2–8.
2. Jacob A, Weinschenker BG. An approach to the diagnosis of acute transverse myelitis. *Semin Neurol*. 2008;28:105–20.
3. Nichtweiß M, Weidauer S. Differential diagnosis of acute myelopathies: an update. *Clin Neuroradiol*. 2015;25(Suppl):183–7.
4. Seidenwurm DJ, Expert Panel on Neurologic Imaging. Myelopathy. *AJNR Am J Neuroradiol*. 2008;29:1032–4.
5. Goh C, Phal PM, Desmond PM. Neuroimaging in acute transverse myelitis. *Neuroimaging Clin N Am*. 2011;21:951–73.
6. Goh C, Desmond PM, Phal PM. MRI in transverse myelitis. *J Magn Reson Imaging*. 2014;40:1267–79.
7. Morales H, Betts A. Abnormal spinal cord magnetic resonance signal: approach to the differential diagnosis. *Semin Ultrasound CT MR*. 2016;37:372–83.
8. West TW, Hess C, Cree BAC. Acute transverse myelitis: demyelinating, inflammatory, and infectious myelopathies. *Semin Neurol*. 2012;32:97–113.
9. Mirbagheri S, Eckart Sorte D, Zamora CA, Mossa-Basha M, Newsome SD, Izbudak I. Evaluation and management of longitudinally

- extensive transverse myelitis: a guide for radiologists. *Clin Radiol*. 2016;71:960–71.
10. Scott TF. Nosology of idiopathic transverse myelitis syndromes. *Acta Neurol Scand*. 2007;115:371–6.
  11. Yiu EM, Kornberg AJ, Ryan MM, Coleman LT, Mackay MT. Acute transverse myelitis and acute disseminated encephalomyelitis in childhood: spectrum or separate entities? *J Child Neurol*. 2009;24:287–96.
  12. The Transverse Myelitis Consortium Working Group Members. Proposed diagnostic criteria and nosology of acute transverse myelitis. *Neurology*. 2002;59:499–505.
  13. Meyer P, Leboucq N, Molinari N, Roubertie A, Carneiro M, Walther-Louvier U, Cuntz-Shadfar D, Leydet J, Cheminal R, Cambonie G, Echenne B, Rondouin G, Deiva K, Mikaeloff Y, Rivier F. Partial acute transverse myelitis is a predictor of multiple sclerosis in children. *Mult Scler*. 2014;20:1485–93.
  14. Lazorthes G. Pathology, classification and clinical aspects of vascular diseases in spinal cord. In: Vinken PJ, Bruyn GW, editors. *Handbook of clinical neurology* vol 12. Amsterdam: North Holland; 1972. pp. 492–506.
  15. Martirosyan N, Feuerstein J, Theodore N, Cavalcanti D, Spetzler R, Preul M. Blood supply and vascular reactivity of the spinal cord under normal and pathological conditions. *J Neurosurg Spine*. 2011;15:238–51.
  16. Thron AK. Vascular anatomy of the spinal cord. *Neuroradiological investigations and clinical syndromes*. Heidelberg Wien New York: Springer; 1988.
  17. Turnbull IM, Brieg A, Hassler O. Blood supply of cervical spinal cord in man. A microangiographic cadaver study. *J Neurosurg*. 1966;24:951–65.
  18. Weidauer S, Nichtweiss M, Lanfermann H, Zanella FE. Spinal cord infarction: MR imaging and clinical features in 16 cases. *Neuroradiology*. 2002;44:851–7.
  19. Weidauer S, Nichtweiß M, Hattingen E, Berkefeld J. Spinal cord ischemia: aetiology, clinical syndromes and imaging features. *Neuroradiology*. 2015;75:241–57.
  20. Yuh WT, Marsh EE 3rd, Wang AK, Russell JW, Chiang F, Koci TM, Ryals TJ. MR imaging of spinal cord and vertebral body infarction. *AJNR Am J Neuroradiol*. 1992;13:145–54.
  21. Vuong SM, Jeong WJ, Morales H, Abruzzo TA. Vascular diseases of the spinal cord: infarction, hemorrhage, and venous congestive myelopathy. *Semin Ultrasound CT MR*. 2016;37:466–81.
  22. Nedeltchev K, Loher TJ, Stepper F, Arnold M, Schroth G, Mattle HP, Sturzenegger M. Longterm outcome of acute spinal cord ischemia syndrome. *Stroke*. 2004;35:560–5.
  23. Tanenbaum LN. Clinical applications of diffusion imaging in the spine. *Magn Reson Imaging Clin N Am*. 2013;21:299–320.
  24. Thurnher MM, Bammer R. Diffusion-weighted MR imaging (DWI) in spinal cord ischemia. *Neuroradiology*. 2006;48:795–801.
  25. Thurnher MM, Law M. Diffusion-weighted imaging, diffusion-tensor imaging, and fiber tractography of the spinal cord. *Magn Reson Imaging Clin N Am*. 2009;17:225–44.
  26. Marcel C, Kremer S, Jeantroux J, Blanc F, Dietemann JL, De Sèze J. Diffusion-weighted imaging in noncompressive myelopathies: a 33-patient prospective study. *J Neurol*. 2010;257:1438–45.
  27. Weidauer S, Gartenschläger M, Claus D. Spinal sulcal artery syndrome due to bilateral vertebral artery dissection. *J Neurol Neurosurg Psychiatry*. 1999;67:550–1.
  28. Caplan LR, Zarins ZK, Hemmati M. Spontaneous dissection of the extracranial vertebral arteries. *Stroke*. 1985;16:1030–8.
  29. Bergqvist C, Goldberg HI, Thorarensen O, Bird SJ. Posterior cervical spinal cord infarction following vertebral artery dissection. *Neurology*. 1997;48:1112–5.
  30. Hundsberger T, Thömke F, Hopf HC, Fitzek C. Symmetrical infarction of the cervical spinal cord due to spontaneous bilateral vertebral artery dissection. *Stroke*. 1998;29:1742.
  31. Pullicino P. Bilateral upper limb amyotrophy and watershed infarcts from vertebral artery dissection. *Stroke*. 1994;25:1870–2.
  32. Richard S, Abdallah R, Chanson A, Foscolo S, Baillot PA, Ducrocq X. Unilateral posterior cervical spinal cord infarction due to spontaneous vertebral artery dissection. *J Spinal Cord Med*. 2014;37:233–6.
  33. Piao YS, Lu DH, Su YY, Yang XP. Anterior spinal cord infarction caused by fibrocartilaginous embolism. *Neuropathology*. 2009;29:172–5.
  34. Tosi L, Rigoli G, Beltramello A. Fibrocartilaginous embolism of the spinal cord: a clinical and pathogenetic reconsideration. *J Neurol Neurosurg Psychiatry*. 1996;60:55–60.
  35. Shuster A, Franchetto A. Surfer's myelopathy – an unusual cause of acute spinal ischemia: a case report and review of the literature. *Emerg Radiol*. 2011;18:57–60.
  36. Hennedige T, Chow W, Ng YY, Chung-Tsing GC, Lim TCC, Kei PL. MRI in spinal cord compression sickness. *J Med Imaging Radiat Oncol*. 2012;56:282–8.
  37. Tanaka H, Minatoya K, Matsuda H, Sasaki H, Iba Y, Oda T, Kobayashi J. Embolism is emerging as a major cause of spinal cord injury after descending and thoracoabdominal aortic repair with a contemporary approach: magnetic resonance findings of spinal cord injury. *Interact Cardiovasc Thorac Surg*. 2014;19:205–10.
  38. Popescu A, Lai D, Lu A, Gardner K. Stroke following epidural injections – case report and review of literature. *J Neuroimaging*. 2013;23:118–21.
  39. Diaz E, Morales H. Spinal cord anatomy and clinical syndromes. *Semin Ultrasound CT MR*. 2016;37:360–71.
  40. Mercier P, Brassier G, Fournier D, Hentati N, Pasco-Papon A, Papon X. Predictability of the cervical origin of the anterior spinal artery. *Interv Neuroradiol*. 1997;20:283–8.
  41. Goldsmith P, Rowe D, Jäger R, Kapoor R. Focal vertebral artery dissection causing Brown – Séquard's syndrome. *J Neurol Neurosurg Psychiatry*. 1998;64:415–6.
  42. Laufs H, Weidauer S, Heller C, Lorenz M, Neumann-Haefelin T. Hemi-spinal cord infarction due to vertebral artery dissection in congenital afibrinogenemia. *Neurology*. 2004;63:1522–3.
  43. Lipper MH, Goldstein JH, Do HM. Brown – Séquard syndrome of the cervical spinal cord after chiropractic manipulation. *AJNR Am J Neuroradiol*. 1998;19:1349–52.
  44. Murata K, Ikeda K, Muto M, Hirajama T, Kano O, Iwasaki Y. A case of posterior spinal artery syndrome in the cervical cord: a review of the clinicoradiological literature. *Intern Med*. 2012;51:803–7.
  45. Kaneki M, Inoue K, Shimizu T, Mannen T. Infarction of the unilateral posterior horn and lateral column of the spinal cord with sparing of posterior columns: demonstration by MRI. *J Neurol Neurosurg Psychiatry*. 1994;57:629–31.
  46. Hathout L, El-Saden S. Nitrous oxide-induced B 12 deficiency myelopathy: perspectives on the clinical biochemistry of vitamin B 12. *J Neurol Sci*. 2011;301:1–8.
  47. Kumar N. Metabolic and toxic myelopathies. *Semin Neurol*. 2012;32:123–36.
  48. Nichtweiß M, Hattingen E, Weidauer S. Metabolic-toxic diseases and atrophic changes of the spinal cord. In: Hattingen E, Weidauer S, Setzer M, Klein J, Vrionis K, editors. *Diseases of the spinal cord – novel imaging, diagnosis and treatment*. Heidelberg: Springer; 2015. pp. 369–87.
  49. Ramalho J, Hoffmann Nunes R, da Rocha AJ, Castillo M. Toxic and metabolic myelopathies. *Semin Ultrasound CT MR*. 2016;37:448–65.
  50. Gelfan S, Tarlov IM. Differential vulnerability of spinal cord structures to anoxia. *J Neurophysiol*. 1955;18:170–88.
  51. Berg D, Mullges W, Klotzenburg M, Bendszus M, Reiners K. Man-in-the-barrel syndrome caused by cervical spinal cord infarction. *Acta Neurol Scand*. 1998;97:417–9.

52. Urban P, Gawehn J, Ringel K. "Man-in-the-barrel" syndrome. *Clin Neuroradiol.* 2005;15:190–4.
53. Leboutoux MV, Franques J, Guillevin R, Delmont E, Lenglet T, Bede P, et al. Revisiting the spectrum of lower motor neuron diseases with snake eyes appearance on magnetic resonance imaging. *Eur J Neurol.* 2014;21:1233–41.
54. Desai JA, Melanson M. Teaching neuroimages: anterior horn cell hyperintensity in Hirayama disease. *Neurology.* 2011;77:e73.
55. Hirayama K. Juvenile muscular atrophy of the upper extremity (Hirayama disease). *Intern Med.* 2000;39:283–90.
56. Kira J, Isobe N, Kawano Y, Osoegawa M, Ohyagi Y, Mihara F, Murai H. Atopic myelitis with focal amyotrophy: a possible link to Hopkins syndrome. *J Neurol Sci.* 2008;269:143–51.
57. Maloney JA, Mirsky DM, Messacar K, Dominguez SR, Schreiner T, Stence NV. MRI findings in children with acute flaccid paralysis and cranial nerve dysfunction occurring during the 2014 Enterovirus D68 outbreak. *AJNR Am J Neuroradiol.* 2015;36:245–50.
58. Krampfl W, Aboul-Enein F, Jecel J, Lang W, Fertl E, Hruby W, Kristoferitsch W. Spinal cord lesions in patients with neuromyelitis optica: a retrospective long-term MRI follow-up study. *Eur Radiol.* 2009;19:2535–43.
59. Nichtweiß M, Hattungen E, Weidauer S. Inflammation of the spinal cord. In: Hattungen E, Weidauer S, Setzer M, Klein J, Vrionis K, editors. *Diseases of the spinal cord – novel imaging, diagnosis and treatment.* Heidelberg: Springer; 2015. pp. 315–68.
60. Yeung SC, Antonio G, Ip KS. Flaccid paralysis of the limbs after an asthmatic attack. *Pediatr Neurol.* 2010;42:133–6.
61. Holland NR. Acute myelopathy with normal imaging. *J Child Neurol.* 2013;28:648–50.
62. Alblas CL, Bouvy WH, Lycklama À, Nijeholt GJ, Boiten J. Acute spinal cord ischemia: evolution of MRI findings. *J Clin Neurol.* 2012;8:218–23.
63. Krings T. Vascular malformations of the spine and spinal cord. *Clin Neuroradiol.* 2010;20:5–24.
64. Atkinson JL, Miller GM, Krauss WE, Marsh WR, Piepgras DG, Atkinson PP, Brown RD Jr, Lane JI. Clinical and radiographic features of dural arteriovenous fistula, a treatable cause of myelopathy. *Mayo Clin Proc.* 2001;76:1120–30.
65. Mull M, Nijenhuis RJ, Backes WH, Krings T, Wilms JT, Thron A. Value and limitations of contrast-enhanced MR angiography in spinal arteriovenous malformations and dural arteriovenous fistulas. *AJNR Am J Neuroradiol.* 2007;28:1249–58.
66. Kimura AI, Tan CF, Wakida K, Saio M, Hozumi I, Inuzuka T, Takahashi H. Venous congestive myelopathy of the cervical spinal cord: an autopsy case showing a rapidly progressive clinical course. *Neuropathology.* 2007;27:284–9.
67. Deiva K, Absoud M, Hemingway C, Hernandez Y, Hussson B, Maurey H, Niotakis G, Wassmer E, Lim M, Tardieu M; United Kingdom Childhood Inflammatory Demyelination (UK-CID) Study and French Kidbiosep Study. Acute idiopathic myelitis in children. Early predictors of relapse and disability. *Neurology.* 2015;84:341–9.
68. Debette S, de Sèze J, Pruvo JP, Zephir H, Pasquier F, Leys D, Vermersch P. Long-term outcome of acute and subacute myelopathies. *J Neurol.* 2009;256:980–8.
69. Rovira A, Auger C. Spinal cord in multiple sclerosis: magnetic resonance imaging features and differential diagnosis. *Semin Ultrasound CT MR.* 2016;37:396–410.
70. Riederer I, Karampinos DC, Settles M, Preibisch C, Bauer JS, Kleine JF, Mühlau M, Zimmer C. Double inversion recovery sequence of the cervical spinal cord in multiple sclerosis and related inflammatory diseases. *AJNR Am J Neuroradiol.* 2015;36:219–25.
71. Tartaglino LM, Friedman DP, Flanders AE, Lublin FD, Knobler RL, Liem M. Multiple sclerosis in the spinal cord: MR appearance and correlation with clinical parameters. *Radiology.* 1995;195:725–32.
72. Wingerchuk DM, Lennon VA, Lucchinetti CF, Pittock SJ, Weinshenker BG. The spectrum of neuromyelitis optica. *Lancet Neurol.* 2007;6:805–15.
73. Trebst C, Raab P, Voss EV, Rommer P, Abu-Mugheisib M, Zettl UK, Stangel M. Longitudinal extensive transverse myelitis – it's not all neuromyelitis optica. *Nat Rev Neurol.* 2011;7:688–98.
74. Eckstein C, Syc S, Saidha S. Differential diagnosis of longitudinally extensive transverse myelitis in adults. *Eur Neurol J.* 2011;3:27–39.
75. Kitley JL, Leite MI, George JS, Palace JA. The differential diagnosis of longitudinally extensive transverse myelitis. *Mult Scler.* 2012;18:271–85.
76. Kitley J, Leite MI, Küker W, Quaghebeur G, George J, Waters P, Woodhall M, Vincent A, Palace J. Longitudinally extensive transverse myelitis with and without aquaporin 4 antibodies. *JAMA Neurol.* 2013;70:1375–81.
77. Birnbaum J, Petri M, Thompson R, Izbudak I, Kerr D. Distinct subtypes of myelitis in systemic lupus erythematosus. *Arthritis Rheum.* 2009;60:3378–87.
78. Kim SM, Waters P, Vincent A, Kim SY, Kim HJ, Hong YH, Park KS, Min JH, Sung JJ, Lee KW. Sjögren's syndrome myelopathy: spinal cord involvement in Sjögren's syndrome might be a manifestation of neuromyelitis optica. *Mult Scler.* 2009;15:1062–8.
79. Al Sawaf A, Berger JR. Longitudinally extensive transverse myelitis suspected for isolated Neuro-Behçet: a diagnostic conundrum. *Mult Scler Relat Disord.* 2015;4:395–9.
80. Yesilot N, Mutlu M, Gungor O, Baykal B, Serdaroglu P, Akman-Demir G. Clinical characteristics and course of spinal cord involvement in Behçet's disease. *Eur J Neurol.* 2007;14:729–37.
81. Kerr DA, Ayetey H. Immunopathogenesis of acute transverse myelitis. *Curr Opin Neurol.* 2002;15:339–47.
82. Eckart Sorte D, Poretti A, Newsome SD, Boltshauser E, Huisman TA, Izbudak I. Longitudinally extensive myelopathy in children. *Pediatr Radiol.* 2015;45:244–57.
83. Young V, Quaghebeur G. Transverse myelitis and neuromyelitis optica spectrum disorders. *Semin Ultrasound CT MR.* 2016;37:384–95.
84. Flanagan EP, Kaufmann TJ, Krecke KN, Aksamit AJ, Pittock SJ, Keegan BM, Giannini C, Weinshenker BG. Discriminating long myelitis of Neuromyelitis Optica from sarcoidosis. *Ann Neurol.* 2016;79:437–47.
85. Marin SE, Callen DJ. The magnetic resonance imaging appearance of monophasic acute disseminated encephalomyelitis: an update post application of the 2007 consensus criteria. *Neuroimaging Clin N Am.* 2013;23:245–66.
86. Huh SY, Min JH, Kim W, Kim SH, Kim HJ, Kim BJ, Kim BJ, Lee KH. The usefulness of brain MRI at onset in the differentiation of multiple sclerosis and seropositive neuromyelitis optica spectrum disorders. *Mult Scler.* 2014;20:695–704.
87. Tackley G, Küker W, Palace J. Magnetic resonance imaging in neuromyelitis optica. *Mult Scler.* 2014;20:1153–64.
88. Wingerchuk DM, Banwell B, Bennett JL, Cabre P, Carroll W, Chitnis T, de Seze J, Fujihara K, Greenberg B, Jacob A, Jarius S, Lana-Peixoto M, Levy M, Simon JH, Tenenbaum S, Traboulsee AL, Waters P, Wellik KE, Weinshenker BG; International Panel for NMO Diagnosis. International consensus diagnostic criteria for neuromyelitis optica spectrum disorders. *Neurology.* 2015;85:177–89.
89. Lucchinetti CF, Guo Y, Popescu BF, Fujihara K, Itoyama Y, Misu T. The pathology of an autoimmune astrocytopathy: lessons learned from neuromyelitis optica. *Brain Pathol.* 2014;24:83–97.
90. Pekcevik Y, Mitchell CH, Mealy MA, Orman G, Lee IH, Scott D. Differentiating neuromyelitis optica from other causes of longitudinally extensive transverse myelitis on spinal magnetic resonance imaging. *Mult Scler.* 2016;22:302–11.
91. Cai W, Tan S, Zhang L, Shan Y, Wang Y, Lin Y. Linear lesions may assist early diagnosis of neuromyelitis optica and longitudinally ex-



- tensive transverse myelitis, two subtypes of NMOSD. *J Neurol Sci.* 2016;360:88–93.
92. Flanagan EP, Weinshenker BG, Krecke KN, Lennon VA, Lucchinetti CF, McKeon A, Wingerchuk DM, Shuster EA, Jiao Y, Horta ES, Pittock SJ. Short myelitis lesions in aquaporin-4-IgG-positive neuromyelitis optica spectrum disorders. *JAMA Neurol.* 2015;72:81–7.
  93. Huh SY, Kim SH, Hyun JW, Jeong IH, Park MS, Lee SH, Kim HJ. Short segment myelitis as a first manifestation of neuromyelitis optica spectrum disorders. *Mult Scler.* 2017;23(3):413–9.
  94. Wingerchuk DM, Weinshenker BG. The emerging relationship between neuromyelitis optica and systemic rheumatologic autoimmune disease. *Mult Scler.* 2012;18:5–10.
  95. Cobo-Calvo Á, Sepúlveda M, Bernard-Valnet R, Ruiz A, Brassat D, Martínez-Yélamos S, Saiz A, Marignier R. Antibodies to myelin oligodendrocyte glycoprotein in aquaporin 4 antibody seronegative longitudinally extensive transverse myelitis: Clinical and prognostic implications. *Mult Scler.* 2016;22:312–9.
  96. Pröbstel AK, Rudolf G, Dormmair K, Collongues N, Chanson JB, Sanderson NS, Lindberg RL, Kappos L, de Seze J, Derfuss T. Anti-MOG antibodies are present in a subgroup of patients with a neuromyelitis optica phenotype. *J Neuroinflammation.* 2015;12:46.
  97. Kitley J, Woodhall M, Waters P, Leite MI, Devenney E, Craig J, Palace J, Vincent A. Myelin-oligodendrocyte glycoprotein antibodies in adults with a neuromyelitis optica phenotype. *Neurology.* 2012;79:1273–7.
  98. van Pelt ED, Wong YYM, Ketelslegers IA, Hamann D, Hintzen RQ. Neuromyelitis optica spectrum disorders: comparison of clinical and magnetic resonance imaging characteristics of AQP4-IgG versus MOG-IgG seropositive cases in the Netherlands. *Eur J Neurol.* 2016;23:580–7.
  99. Kastenbauer S, Winkler F, Fesl G, Schiel X, Ostermann H, Yousry TA, Pfister HW. Acute severe spinal cord dysfunction in bacterial meningitis in adults. MRI findings suggest extensive myelitis. *Arch Neurol.* 2001;58:806–10.
  100. Okada S, Chang C, Chang G, Yue J. Venous hypertensive myelopathy associated with cervical spondylosis. *Spine J.* 2016;16:e751–e4.
  101. Flanagan EP, Krecke KN, Marsh RW, Giannini C, Keegan BM, Weinshenker BG. Specific pattern of gadolinium enhancement in spondylotic myelopathy. *Ann Neurol.* 2014;76:54–65.
  102. Polman CH, Reingold SC, Banwell B, Clanet M, Cohen JA, Filippi M, Fujihara K, Havrdova E, Hutchinson M, Kappos L, Lublin FD, Montalban X, O'Connor P, Sandberg-Wollheim M, Thompson AJ, Waubant E, Weinshenker B, Wolinsky JS. Diagnostic criteria for multiple sclerosis: 2010 revisions to the McDonald criteria. *Ann Neurol.* 2011;69:292–302.
  103. Gass A, Rocca MA, Agosta F, Ciccarelli O, Chard D, Valsasina P, Brooks JC, Bischof A, Eisele P, Kappos L, Barkhof F, Filippi M; MAGNIMS Study Group. MRI monitoring of pathological changes in the spinal cord in patients with multiple sclerosis. *Lancet Neurol.* 2015;14:443–54.
  104. Thorpe JW, Kidd D, Kendall BE, Tofts PS, Barker GJ, Thompson AJ, MacManus DG, McDonald WI, Miller DH. Spinal cord MRI using multi-array coils and fast spin echo. 1. Technical aspects and findings in healthy adults. *Neurology.* 1993;43:2625–31.
  105. Oppenheimer DR. The cervical cord in multiple sclerosis. *Neuropath Appl Neurobiol.* 1978;4:151–62.
  106. Wagner M, Klein JC. Meningeal disorders. In: Hattingen E, Weidauer S, Setzer M, Klein J, Vrionis K, editors. *Diseases of the spinal cord – novel imaging, diagnosis and treatment.* Heidelberg: Springer; 2015. pp. 271–99.
  107. Deshayes S, Bonhomme J, de La Blanchardière A. Neurotoxocarisis: a systematic literature review. *Infection.* 2016;44:565–74.
  108. Singer OC, Conrad F, Jahnke K, Hattingen E, Auer H, Steinmetz H. Severe meningoencephalitis due to CNS toxocarosis. *J Neurol.* 2011;258:696–8.
  109. Devinsky O, Cho ES, Petit CK, Price RW. Herpes Zoster myelitis. *Brain.* 1999;114:1181–96.
  110. Hosaka A, Nakamagoe K, Watanabe M, Tamaoka A. Magnetic resonance images of herpes zoster myelitis presenting with Brown-Séquard syndrome. *Arch Neurol.* 2010;67:506–7.
  111. Flanagan EP, McKeon A, Lennon VA, Kearns J, Weinshenker BG, Krecke KN, Matiello M, Keegan BM, Mokri B, Aksamit AJ, Pittock SJ. Paraneoplastic isolated myelopathy: clinical course and neuroimaging clues. *Neurology.* 2011;76:2089–95.
  112. Flanagan EP, Keegan BM. Paraneoplastic myelopathy. *Neurol Clin.* 2013;31:307–18.
  113. Scaravilli F, Bazille C, Gray F. Neuropathologic contributions to understanding AIDS and the central nervous system. *Brain Pathol.* 2007;17:197–208.
  114. Hatanpaa KJ, Kim JH. Neuropathology of viral infections. In: Tselis AC, Booss J, editors. *Neurovirology Handbook of Clinical Neurology*, (3rd series), vol 123. Amsterdam: Elsevier; 2014. pp. 193–214.
  115. Weidauer S, Nichtweiß M, Hattingen E. Differential diagnosis of white matter lesions: non vascular causes – part II. *Clin Neuroradiol.* 2014;24:93–110.